Bioresource Technology 372 (2023) 128659

Contents lists available at ScienceDirect

Bioresource Technology

journal homepage: www.elsevier.com/locate/biortech

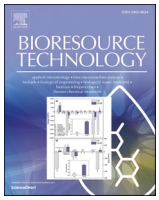

Microbial dynamics and bioreactor performance are interlinked with organic matter removal from wastewater treatment plant effluent

M. Atasoy [a,b,c,*], W.T. Scott Jr. [a,d], K. van Gijn [b], J.J. Koehorst [a,d], H. Smidt [a,c], A.A.M. Langenhoff [a,b]

[a] UNLOCK, Wageningen University & Research and Technical University Delft, Wageningen and Delft, The Netherlands
[b] Department of Environmental Technology, Wageningen University & Research, PO box 8129, 6700 EV, Wageningen, The Netherlands
[c] Laboratory of Microbiology, Wageningen University & Research, The Netherlands
[d] Laboratory of Systems and Synthetic Biology, Wageningen University & Research, The Netherlands

HIGHLIGHTS

- Bioreactor performance and microbial community profile were interdependent.
- *Proteobacteria* was the most predominant phylum in all bioreactors.
- Relative abundance of *Roseococcus* correlated with organic matter removal.
- The incremental flow rate changes affected microbial community composition.
- The gLV model identified relations within the microbial community.

GRAPHICAL ABSTRACT

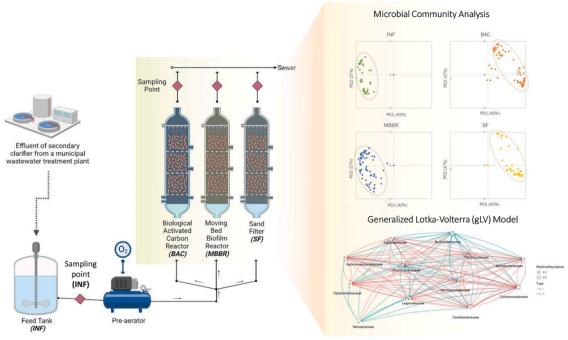

ARTICLE INFO

Keywords:
Microbial community profile
generalized Lotka-Volterra (gLV) model
Biological activated carbon bioreactor
Moving bed biofilm reactor
Sand filter

ABSTRACT

Optimizing bioreactor performance for organic matter removal can achieve sustainable and energy-efficient micropollutant removal in subsequent tertiary treatment. Bioreactor performance heavily depends on its resident microbial community; hence, a deeper understanding of community dynamics is essential. The microbial communities of three different bioreactors (biological activated carbon, moving bed biofilm reactor, sand filter), used for organic matter removal from wastewater treatment effluent, were characterized by 16S rRNA gene amplicon sequence analysis. An interdependency between bioreactor performance and microbial community profile was observed. Overall, *Proteobacteria* was the most predominant phylum, and *Comamonadaceae* was the most predominant family in all bioreactors. The relative abundance of the genus *Roseococcus* was positively correlated with organic matter removal. A generalized Lotka-Volterra (gLV) model was established to understand the interactions in the microbial community. By identifying microbial dynamics and their role in bioreactors, a strategy can be developed to improve bioreactor performance.

* Corresponding author.
E-mail address: merve.atasoy@wur.nl (M. Atasoy).

https://doi.org/10.1016/j.biortech.2023.128659
Received 12 December 2022; Received in revised form 17 January 2023; Accepted 18 January 2023
Available online 20 January 2023
0960-8524/© 2023 The Author(s). Published by Elsevier Ltd. This is an open access article under the CC BY license (http://creativecommons.org/licenses/by/4.0/).

1. Introduction

The transformation of conventional wastewater treatment plants (WWTPs) into energy-efficient and sustainable WWTPs is essential for achieving Sustainable Development Goals 12 (responsible consumption and production) and 13 (climate action) (United Nations, 2018). In this regard, energy-intensive treatment methods should be optimized by reducing greenhouse gas emissions and, thus, their carbon footprint while still meeting discharge limits. Nevertheless, the removal of some compounds, including micropollutants, e.g., pharmaceuticals, pesticides, and personal care products, at WWTPs is to date mainly ensured by energy-intensive tertiary treatments (e.g., ozonation, membrane filtration, catalyzed UV treatment). The micropollutant removal efficiency by these treatments is negatively correlated with the amount of organic matter (OM). In other words, a lower organic matter content in the tertiary treatment reduces energy consumption and improves micropollutant removal efficiency (Nilsson et al., 2017; van Gijn et al., 2021). Therefore, van Gijn et al. (2021) aimed to optimize organic matter removal by using either a biological activated carbon bioreactor (BAC), a moving bed biofilm reactor (MBBR), or a sand filter (SF) as a pre-treatment step for subsequent micropollutant removal (van Gijn et al., 2021). Organic matter removal efficiency varied between the bioreactors (i.e., BAC 72 %, SF 41 %, and MBBR 21 %) (van Gijn et al., 2021). Microbial communities residing in these bioreactors have a profound effect on their performance. Primarily, specific compound removal efficiency is associated with microbial community composition (Chen et al., 2021). However, to optimize bioreactor performance, it is crucial to understand microbial community profiles, interactions between community members, and their functions.

16S ribosomal RNA (rRNA) gene amplicon sequencing is currently the most widely used method for compositional profiling of microbial community composition. It has repeatedly been demonstrated as an effective means for that purpose (Kodera et al., 2022). Going a step further, systems biology-based modeling techniques have recently been used to elucidate microbial co-occurrence patterns to infer emergent properties within microbial communities (van den Berg et al., 2022). These techniques range from correlation-based methods to complex network models (Barberán et al., 2012; Gross et al., 2010; Lu et al., 2022). Among these techniques, a popular method using few parameters and differential equations, generalized Lotka-Volterra (gLV) modeling, has been used to estimate growth rates and infer interaction strengths among taxa within a microbial community (Bucci et al., 2016; Li et al., 2021).

In the current study, microbial community composition was analyzed using 16S rRNA gene amplicon sequencing to assess whether there is a link between microbial composition and bioreactor performance. Moreover, we applied a recent gLV modeling approach (Li et al., 2021) to capture operational taxonomic unit (OTU) dynamics and help deduce the network structure of the microbial communities from the various bioreactors (i.e., BAC, MBBR, and SF) and influent (INF). gLV modeling is a powerful approach for predicting microbial interactions in ecosystems, although its intrinsic limitations should be considered when interpreting the outcome. Firstly, gLV modeling contains a static interaction matrix that might not fully capture shifts in interactions within a community (Momeni et al., 2017). Secondly, gLV modeling only contains pairwise interactions, thus, missing the capacity to factor potential higher-order interactions among taxa (Mickalide and Kuehn, 2019). Thirdly, metabolite-mediated interactions are not explicitly contained in gLV models (Zomorrodi and Segrè, 2016). Although gLV models solely may thus not be able to comprehensively interpret community-level behavior, the current study greatly benefits from the gLV model for describing context-specific interactions in the bioreactors.

As a follow-up study of van Gijn et al (2021), in this study, we have studied microbial dynamics in three bioreactors (BAC, MBBR, and SF) and their association with bioreactor performance by employing 16S rRNA gene amplicon sequencing and the gLV model. In addition, we assessed the effects of different flow rates and sampling strategies (i.e., short-term hourly vs longer-term daily sampling) on microbial dynamics.

2. Materials and methods

The current study is a follow-up to the study of van Gijn et al. (2021), and detailed information regarding the experimental setup, bioreactor operation, substrate characterization, inoculum, and analytical methods can be found in van Gijn et al. (2021). Briefly, a mixture of biologically activated sludges from four different WWTPs (the Netherlands) was used as an inoculum source. The effluent from the secondary clarifier of a WWTP (Bennekom, the Netherlands) was used as substrate. It contained 24 mg/L of chemical oxygen demand (COD), 7 mg/L of total organic carbon (TOC), 9.02 mg/L of nitrate, and 0.57 mg/L of total phosphate. Three bioreactors (BAC, MBBR, and SF) with a total volume of 1.7 L each were operated aerobically in a continuous mode. A pre-aerator was used to add pure oxygen to the influent of each bioreactor to ensure aerobic conditions. However, the dissolved oxygen (DO) concentration varied according to the type and hydraulics of the bioreactor throughout bioreactor operation. DO was 30 mg/L in the MBBR, whereas it was 19 mg/L on average (min 2 and max 36 mg/L) in the SF and 9 mg/L on average (min 1 and max 30 mg/L) in the BAC (van Gijn et al., 2021). The bioreactor performance was monitored by UV254 absorbance, COD, and TOC analyses. Furthermore, the concentrations of DO, nitrite, nitrate, and total phosphate were monitored. The used micropollutant mix was comprised of pharmaceuticals, pesticides, and industrial-based chemicals (benzotriazole). These micropollutants were chosen based on their presence in the WWTP effluent. A mixture of 16 different micropollutants was spiked into the influent (INF) to obtain a final concentration of 2 μg/L of each micropollutant (van Gijn et al., 2021). After the spike, micropollutant concentrations were measured in the 12th week, and microbial community sampling began afterwards. The specific effects of microbial community profile on individual micropollutant removal were not examined in this study.

2.1. Sampling strategy

Microbial community samples were collected from the feeding tank (influent, INF) and the effluent of each bioreactor (BAC, MBBR, and SF) on a daily or hourly basis (Fig. 1.a). The daily sampling was conducted for flow rates of 1, 0.5, 0.25, 2, 4, 0.25, 1 L/h, whereas hourly sampling was conducted for transition flow rates (L/h) of 1 – 0.5, 0.5 – 0.25, 0.25 – 2, 2 – 4, 4 – 0.25 L/h (Fig. 1.b). The feeding tank was filled four times during bioreactor operation (September 16th, September 23rd, October 16th, and November 13th, 2019) with the effluent of the secondary clarifier of a WWTP. For all liquid samples, a 50 mL sample was filtered with a sterile 0.2 μm filter. The filter was stored in a 2 mL sterile microcentrifuge tube at −80°C until DNA extraction.

2.2. Microbial community analysis

The microbial community was analyzed by Illumina sequencing of the 16S rRNA gene as described by Zhang et al. (2022). Total DNA was extracted by using the DNeasy PowerSoil Kit (QIAGEN, Hilden, Germany) following the manufacturer's instructions. DNA concentrations were measured by Qubit (Thermo Fisher Scientific). 16S rRNA gene fragments were amplified using primers 515F (5′–3′: GTG CCA GCM GCC GCG GTAA) and 806R (5′–3′: GGA CTA CHV GGG TWT CTA AT) (Caporaso et al., 2011; Klindworth et al., 2013) that were amended at the 5′-end with sample-specific barcodes. The PCR mixture (50 μL) was prepared with 10 μL 5 × HF Green buffer (Thermo Fisher Scientific, the Netherlands), 1 μL (2 U) of Phusion hot start II High-Fidelity DNA polymerase (Thermo Fisher Scientific), primer mix (500 nM for each forward and reverse primer), and 500 nM dNTP (Promega, USA), 10 ng DNA template and nuclease-free water (Promega, USA). The PCR

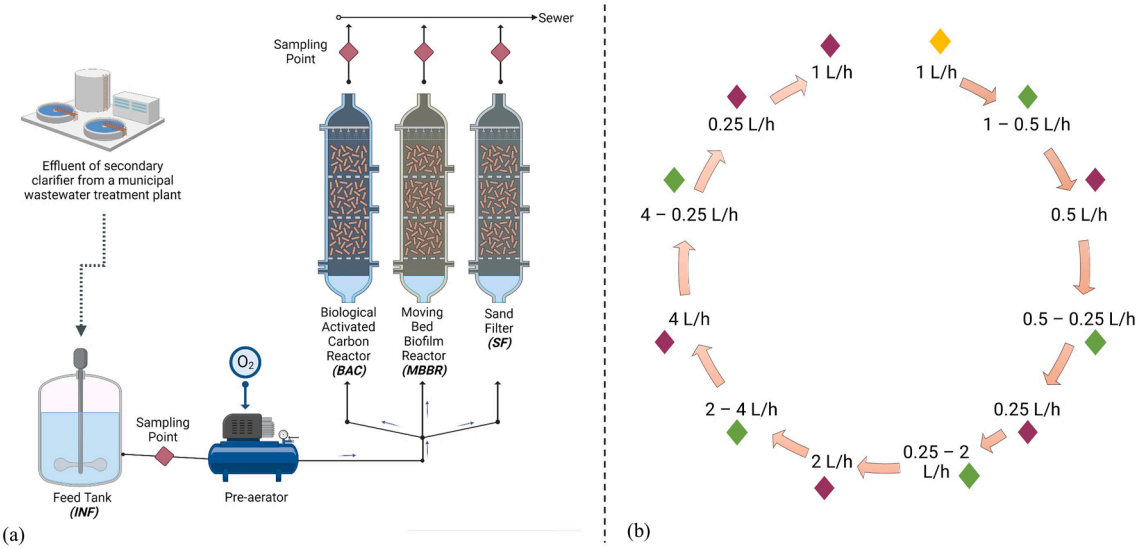

Fig. 1. Illustration of the sampling points (a) based on the reactor configurations: feeding tank (INF); biological activated carbon (BAC) filter; moving bed biofilm reactor (MBBR) and sand filter (SF), and (b) starting point:, hourly: and daily: sampling points based on gradual changes in the flow rate (from 0.25 L/h to 4 L/h).

program was as follows: 98 °C, 30 s for pre-denaturation, followed by 25 cycles of 98 °C, 10 s for denaturation, annealing at 50 °C for 10 s, elongation at 72 °C for 10 s, and a final extension at 72 °C for 7 min. The PCR products were pooled and purified using CleanPCR (cleanNA, the Netherlands) according to the manufacturer's instructions. The purified amplicons were pooled in equimolar amounts, and nuclease-free water as a negative control, and sent for sequencing by Hiseq2000 (GATC-Biotech GmbH, now part of Eurofins Genomics Germany GmbH, Konstanz, Germany).

2.3. Computational analysis

After data registration, the computational workflow was executed (Koehorst and Nijsse, 2021). The quality of the samples was identified using FASTQC, and amplicon sequencing variants (ASVs) were identified and classified using NGTax 2.0 in combination with the Silva 138.1 database (Poncheewin et al., 2020). In order to avoid the inclusion of spurious ASVs caused by sequencing and PCR errors, a threshold of 0.1 % relative abundance was applied per sample. Overall, 12,910,454 reads from 275 samples were used.

2.3.1. Generalized Lotka-Volterra (gLV) modeling

In this study, the BEEM-Static generalized Lotka Volterra (gLV) framework (Li et al., 2021) was applied. The gLV model is a system of ordinary differential equations representing the instantaneous growth rate of each taxon ($dx_i(t)/dt$) as a function of absolute cell densities ($x_i(t)$) of the p taxa in a community. In inferring interactions, the gLV is used in its discrete form, where each time point represents a sample in the time-based abundance profile. The differential equations describe the difference of a single taxon abundance in family level in two adjacent time points, and how it is dependent on the growth rate and its interaction coefficients with the other OTUs.

$$\frac{dx_i(t)}{dt} = \mu_i x_i(t) + \sum_{j=1}^{p} \beta_{ij} x_i(t) x_j(t) \tag{1}$$

Eq. (1) $x_i(t)$ describes the relative abundance of the i^{th} OTU at time t. The growth rate of the i^{th} OTU is described by μ_i. $\boldsymbol{\beta}$ is the overall interspecific interaction matrix, where $\boldsymbol{\beta}_{ij}$ describes the strength of the influence of the j^{th} OTU by the i^{th} OTU. ($\boldsymbol{\beta}_{ij} < 0$ represents a negative effect on the j^{th} OTU by the i^{th} OTU). In general, estimating gLV parameters (μi and βij) requires longitudinal data to measure $dx_i(t)/dt$. However, at the non-trivial equilibrium ($dx_i(t)/dt = 0$ and $x_i > 0$):

$$\mu_i + \sum_{j=1}^{p} \beta_{ij} x_j = 0 \tag{2}$$

this causes the variable time (t) become embedded in the equation. Furthermore, dividing both sides by -βii and the biomass m and further rearrangement, the following term is obtained:

$$\widetilde{x}_i = \frac{a_i}{m} + \sum_{j=1, j\neq i}^{p} b_{ij} \widetilde{x}_j \tag{3}$$

where $a_i = -\mu_i/\beta_{ii}$, $b_{ij} = -\beta_{ij}/\beta_{ii}$ and is the relative abundance of species i at equilibrium (a_i is also known as the carrying capacity of the species). This equation allows BEEM-STATIC to estimate gLV parameters (via a_i and b_{ij}) from cross-sectional data, considering that samples are at equilibrium, and absolute abundances are known ($x_i = m\widetilde{x}_i$) However, since our data does not contain biomass measurements and only contains relative abundances, we employed an extension in BEEM-Static using an EM framework to jointly estimate model parameters and biomass (for more details, see the supplementary section in (Li et al., 2021)).

For estimating the biomass per taxa (i), BEEM-Static acquires the median for each taxa across species as a robust estimator of the biomass from each sample:

$$m^{(T)} = median\left(-\frac{a_i^{(T-1)}}{\sum_{j=1}^{p} b_{ij}^{(T-1)} \widetilde{x}_j} \right) \tag{4}$$

For estimating the model parameters $\left(a_i^{(T)} \text{ and } b_{ij}^{(T)}\right)$ for each i with sparse regression at iteration T:

$$\widetilde{x}_i \quad \frac{1}{m^{(T)}} \bullet a_i^{(T)} + \sum_{j=1,\ j\neq i}^{p} b_{ij}^{(T)} \widetilde{x}_j \tag{5}$$

We used the above BEEM-Static framework as it is in our implementation. Moreover, BEEM-Static statistical filters were used to identify and remove sample that violate modelling assumptions. The equilibrium filter screens for samples that may not be at equilibrium. The equilibrium filter was set to $\epsilon_1 = 20$ % (where $(median\left(\left| \widetilde{x}_i - \widetilde{x}_i^{*} \right| / \widetilde{x}_i \right) \rangle \epsilon_1, \widetilde{x}_i \neq 0$). The model filter screens samples that may originate from an alternate gLV model. The model filter was set to the default value of $\epsilon_2 = 3$ (where $(e_k - \text{median}(e_k))/\text{IQR}(e_k) > \epsilon_2$),

IQR indicates inter-quartile range).

All the abundance values were normalized for each time point. The area under the receiver operating characteristic curve (AUC-ROC) was computed for the interaction matrix Z-scores were used to rank interactions (off-diagonal entries only) predicted by BEEM-Static. Sensitivity for predicting the signs of interaction was calculated as the fraction of interactions with correctly predicted signs in the true interaction matrix (non-zero off-diagonal entries only).

2.3.2. Statistical analysis

Principal Component Analysis (PCA) was applied to the microbial community data to discriminate the samples according to the flow rate as a function of time for each bioreactor type. Pearson's correlation analysis was conducted to identify the relationship between the relative abundance at the family level and the organic matter removal rate (COD, TOC, and UV254). To analyze the shift in microbial community composition, one-way multivariate ANOVA was conducted using the first two principal components; PC1 and PC2, based on relative abundances at the family level and organic matter removal based on time and flow rate. Lastly, PC1 and PC2 were used to conduct the Kolmogorov-Smirnov (K-S) test to understand how well microbial community shifts could be studied based on the sampling structure (hourly and daily). All

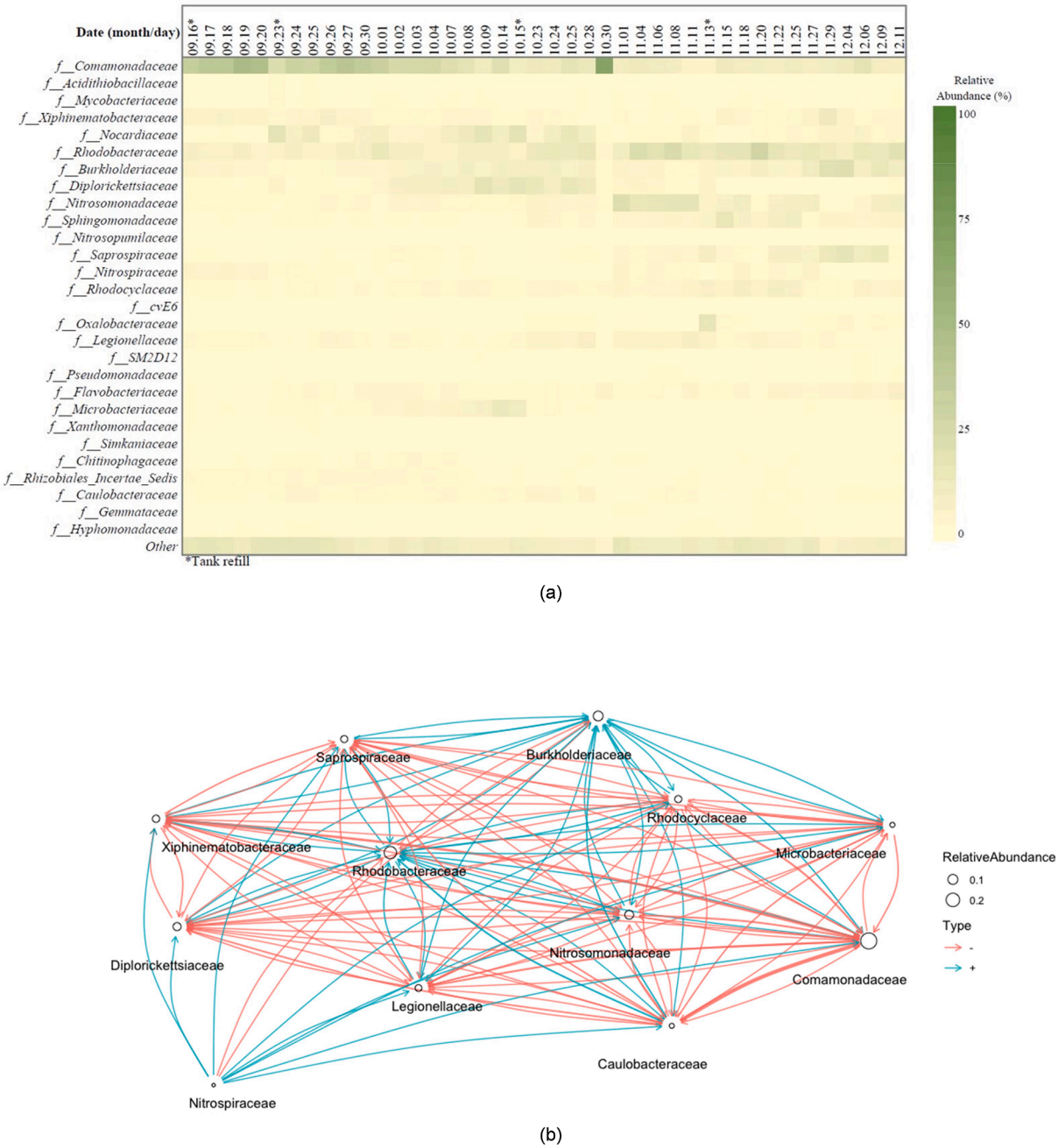

Fig. 2. **(a)** The relative abundance of the family-level microbial community in influent (INF), which is represented with a heat map using daily and hourly sampling regimes, and **(b)** the correlations between the most abundant species are represented with the non-zero interaction terms in gLV model. In the heat map, the color scale varies from absence (white: 0%) to high relative abundance (green: 100%). BEEM-estimated biomass values for INF with daily sampled microbial time series datasets. Graphs representing non-zero interaction terms in gLV models learned individually for the dataset using BEEM. Blue and red edges represent positive and negative interactions, respectively. Edge widths are proportional to the interaction strength, and node sizes are proportional to the log-transformed mean relative abundance of the corresponding species. Nodes are labeled with the most specific taxonomic annotations.

statistical tests were conducted using IBM SPSS Statistics, Version 25.0. The relative abundance heatmaps at the family level were generated using OriginPro, Version Number 2021.

2.4. Data FAIRification

FAIR ENA data submission files were generated using the FAIR Data Station (Nijsse et al., 2022) with the wastewater sludge package information model from ENA (Retrieved 22–08-2022). ENA Project accession number is PRJEB54921. Experimental data and metadata of the project, experimental procedures, samples, and datasets were registered according to the wastewater sludge package (MIxS) using the FAIR Data Station (Yilmaz et al., 2011).

3. Results and discussion

The residing microbial community and its functions play a crucial role in bioreactor performance. While determining the relationship between bioreactor performance and microbial community profile poses several challenges due to the complex interactions between the operational and environmental parameters with the microbial community, molecular tools, and dynamic models can provide valuable insights into it. As a follow-up to van Gijn et al. (2021), the current study investigates the relationship between bioreactor performance and the microbial community profile by considering bioreactor type, flow rate, and sampling strategy. Moreover, gLV modeling was used to identify the strength of interactions among taxa in the observed microbial communities.

3.1. The relation between bioreactor type and microbial community profile

The microbial community profile in the influent, BAC, MBBR, and SF were regularly observed by 16S rRNA gene amplicon sequencing. In terms of organic matter removal efficiency, the highest removal performance for the different bioreactors was 72 % for BAC, 41 % for SF and 21 % for MBBR (van Gijn et al., 2021). The 16S rRNA gene amplicon sequence data at family level (Fig. 2.a, 3.a, 4.a, and 5.a) and its PCA distribution (Fig. 6) indicated that microbial community profiles were related to bioreactor performance. The low performance of the MBBR

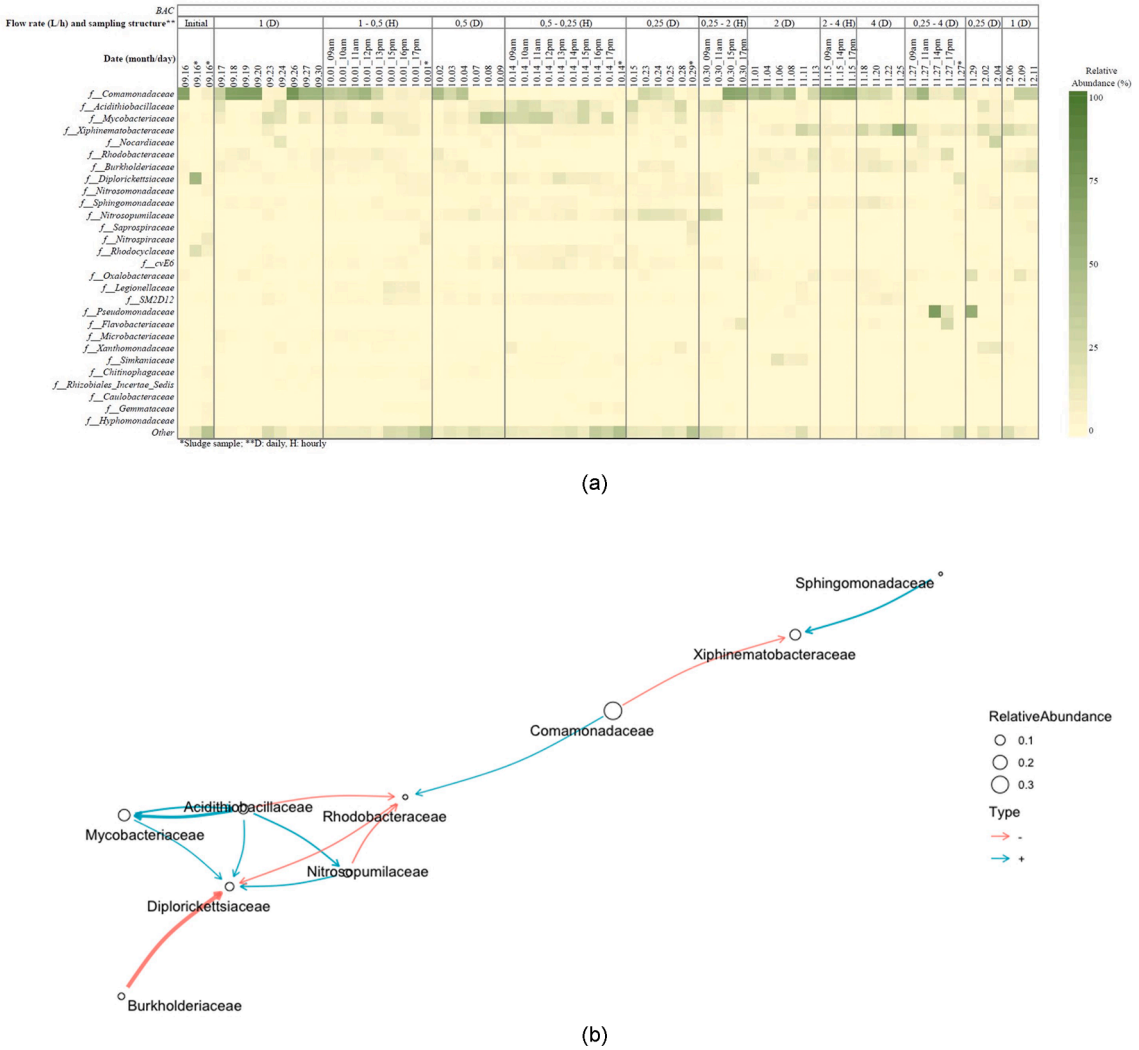

Fig. 3. **(a)** The relative abundance of the family-level microbial community in BAC, which is represented with a heat map using daily and hourly sampling regimes, and **(b)** the correlations between the most abundant species are represented with the non-zero interaction terms in gLV model. In the heat map, the color scale varies from absence (white: 0%) to high relative abundance (green: 100%). BEEM-estimated biomass values for BAC with daily sampled microbial time series datasets. Graphs representing non-zero interaction terms in gLV models learned individually for the dataset using BEEM. Blue and red edges represent positive and negative interactions, respectively. Edge widths are proportional to the interaction strength, and node sizes are proportional to the log-transformed mean relative abundance of the corresponding species. Nodes are labeled with the most specific taxonomic annotations.

coincided with a high similarity between microbial community profiles in the influent and the effluent of the MBBR. By contrast, the effluent of the BAC and SF showed different microbial community profiles compared to the influent. Moreover, this finding was partially aligned with the results of the gLV model (Fig. 2.b, 3.b, 4.b, and 5.b). The gLV model highlights parallels in the dynamics of the influent and MBBR bioreactor microbial communities involved in the complex interactions of its members.

At the phylum level (see Supplementary Fig. 1), the most abundant taxa were *Proteobacteria* (27 ± 10 %), *Cyanobacteria* (26 ± 16 %), and *Bacteroidota* (11 ± 7 %) in the influent. Based on the bioreactor type, the most abundant phyla differed slightly between bioreactors: *Proteobacteria* (44 ± 25 %), *Actinobacteria* (15 ± 13 %), and *Verrumicrobiota* (12 ± 10 %) in the BAC, *Proteobacteria* (24 ± 11 %), *Cyanobacteria* (23 ± 17 %), and *Actinobacteria* (12 ± 10 %) in the MBBR, and *Proteobacteria* (42 ± 24 %), *Actinobacteria* (17 ± 11 %), and *Verrumicrobiota* (9 ± 5 %) in the SF, respectively. However, at the family level, the microbial composition was more distinct between the influent and bioreactor types: *Comamonadaceae* (21 ± 14 %), *Rhodobacteraceae* (12 ± 5 %), *Burkholderiaceae* (7 ± 4 %) were the three most abundant families in the influent (Fig. 2.a); *Comamonadaceae* (24 ± 22 %), *Mycobacteriaceae* (10 ± 7 %), *Xiphinematobacteraceae* (9 ± 5 %) in the BAC (Fig. 3.a), *Comamonadaceae* (15 ± 8 %), *Rhodobacteraceae* (14 ± 11 %), *Nocardiaceae* (7 ± 4 %) in the MBBR (Fig. 4.a) and *Comamonadaceae* (21 ± 14 %), *Acidithiobacillaceae* (16 ± 12 %), *Xiphinematobacteraceae* (6 ± 4 %) in the SF (Fig. 5.a). E-supplementary data for this work can be found in the e-version of this paper online.

Microbial community composition in bioreactors is generally shaped by several factors, including, among others, influent characteristics, inoculum source, bioreactor type, operational conditions, and environmental parameters (Valentín-Vargas et al., 2012). Comparing different studies from a microbial community perspective can be difficult due to these variable factors, but it can also unveil relevant species' functions and their association with bioreactor performance. For instance, Duc

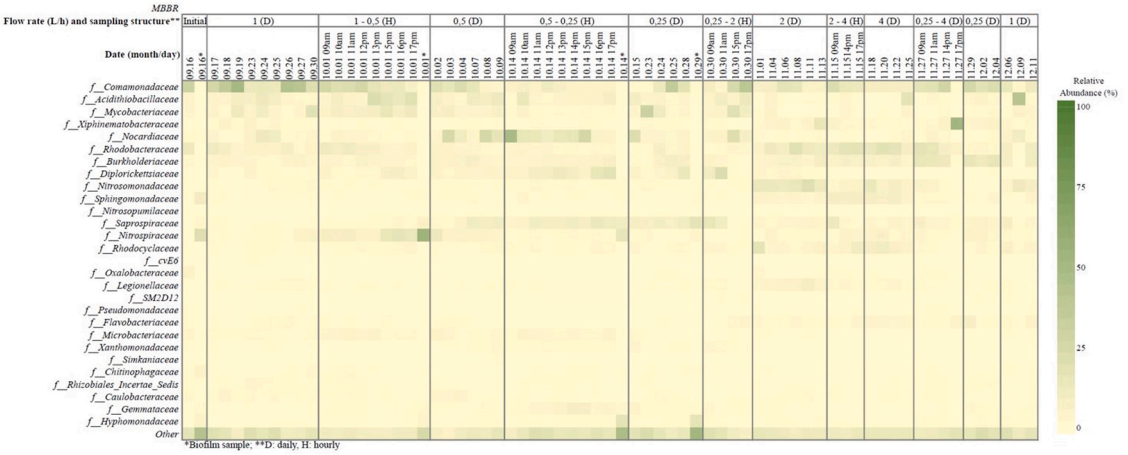

(a)

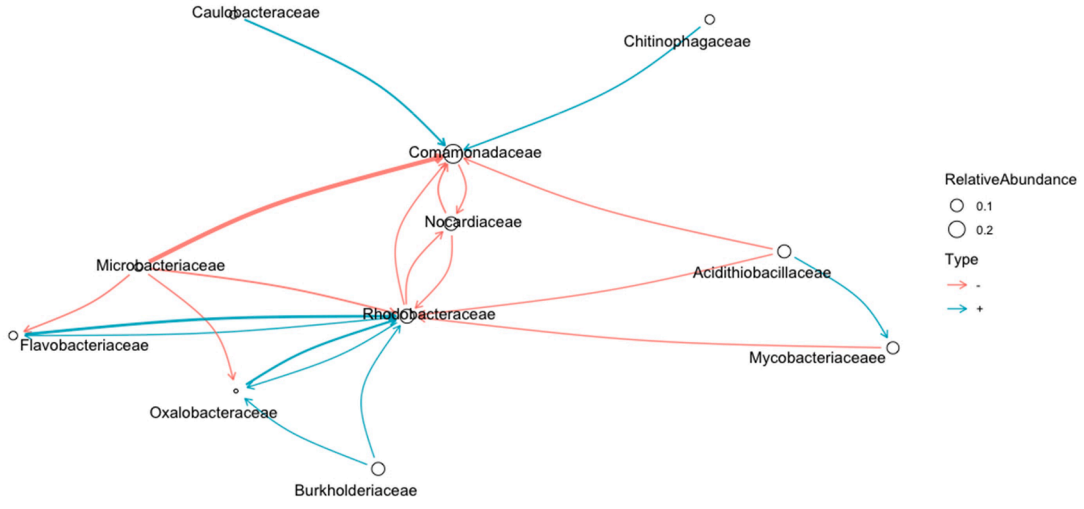

(b)

Fig. 4. **(a)** The relative abundance of the family-level microbial community in MBBR, which is represented with a heat map using daily and hourly sampling regimes and **(b)** the correlations between the most abundant species are represented with the non-zero interaction terms in gLV model. In the heat map, the color scale varies from absence (white: 0%) to high relative abundance (green: 100%). BEEM-estimated biomass values for MBBR with daily sampled microbial time series datasets. Graphs representing non-zero interaction terms in gLV models learned individually for the dataset using BEEM. Blue and red edges represent positive and negative interactions, respectively. Edge widths are proportional to the interaction strength, and node sizes are proportional to the log-transformed mean relative abundance of the corresponding species. Nodes are labeled with the most specific taxonomic annotations.

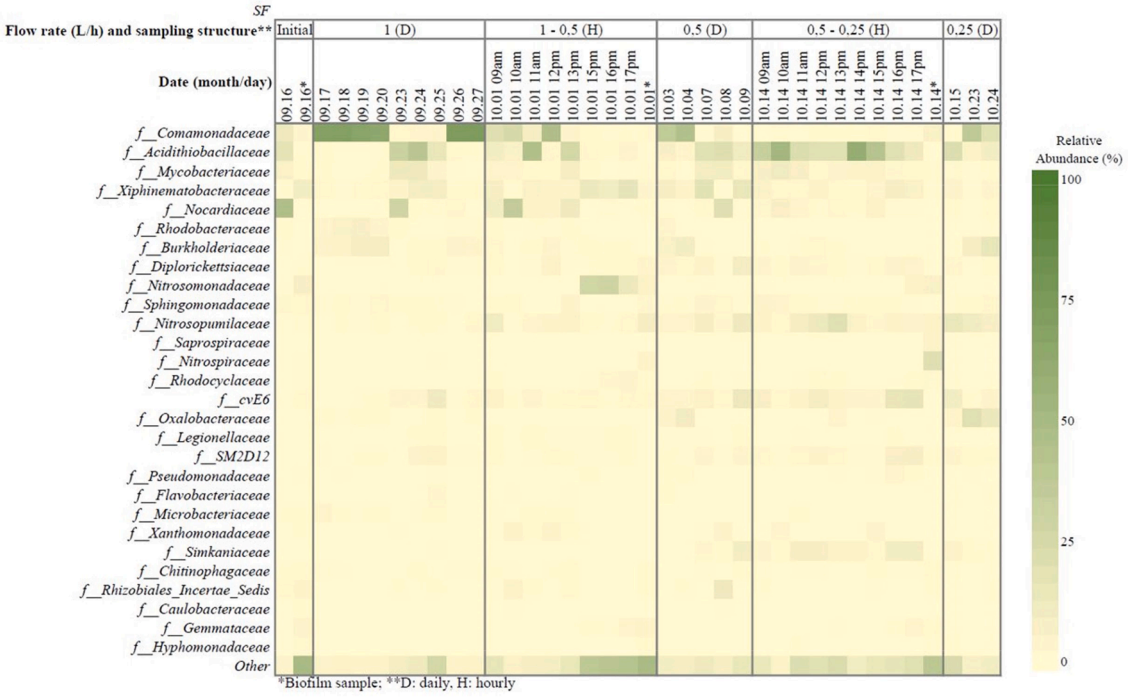

(a)

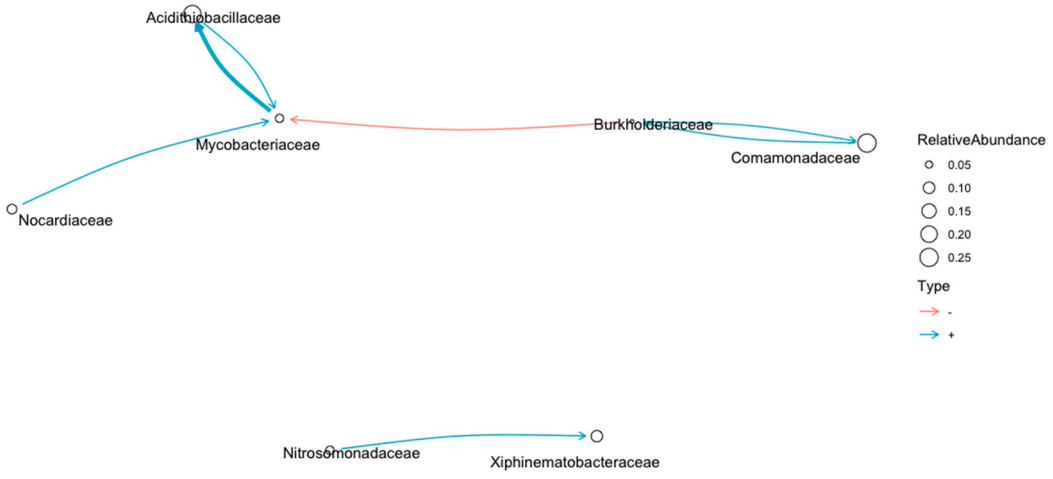

(b)

Fig. 5. **(a)** The relative abundance of the family-level microbial community in SF is represented with a heat map using daily, and hourly sampling regimes, and **(b)** the correlations between the most abundant species are represented with the non-zero interaction terms in gLV model. In the heat map, the color scale varies from absence (white: 0%) to high relative abundance (green: 100%). BEEM-estimated biomass values for SF with daily sampled microbial time series datasets. Graphs representing non-zero interaction terms in gLV models learned individually for the dataset using BEEM. Blue and red edges represent positive and negative interactions, respectively. Edge widths are proportional to the interaction strength, and node sizes are proportional to the log-transformed mean relative abundance of the corresponding species. Nodes are labeled with the most specific taxonomic annotations.

Viet et al. (2022) showed that *Proteobacteria*, *Bacteroidota,* and *Acidobacteriota* were the main phyla (80 %) for degrading organic components in an integrated activated carbon-fertilizer drawn osmotic membrane bioreactor. Moreover, Li et al. (2022) compared the microbial community composition for micropollutant and organic matter removal in different membrane biofilm bioreactors from several studies. *Proteobacteria* was the most predominant phylum for the degradation of chlorinated aromatic compounds (e.g., pentachlorophenol) and the removal of ammonia and organic carbon in an O_2-based membrane biofilm bioreactor (Li et al., 2022). In our study, *Proteobacteria* was predominant in all bioreactors; however, organic matter removal efficiency varied greatly among them. To comprehend the effects of microbial community profiles on micropollutant degradation and organic matter removal, lower taxonomic ranks and/or functional gene repertoires need to be analyzed.

The most predominant family in all bioreactors was *Comamonadaceae*, which belongs to the *Burkholderiales* order in the *Betaproteobacteria* class of the phylum *Proteobacteria* (Brenner et al., 2005). Most of the

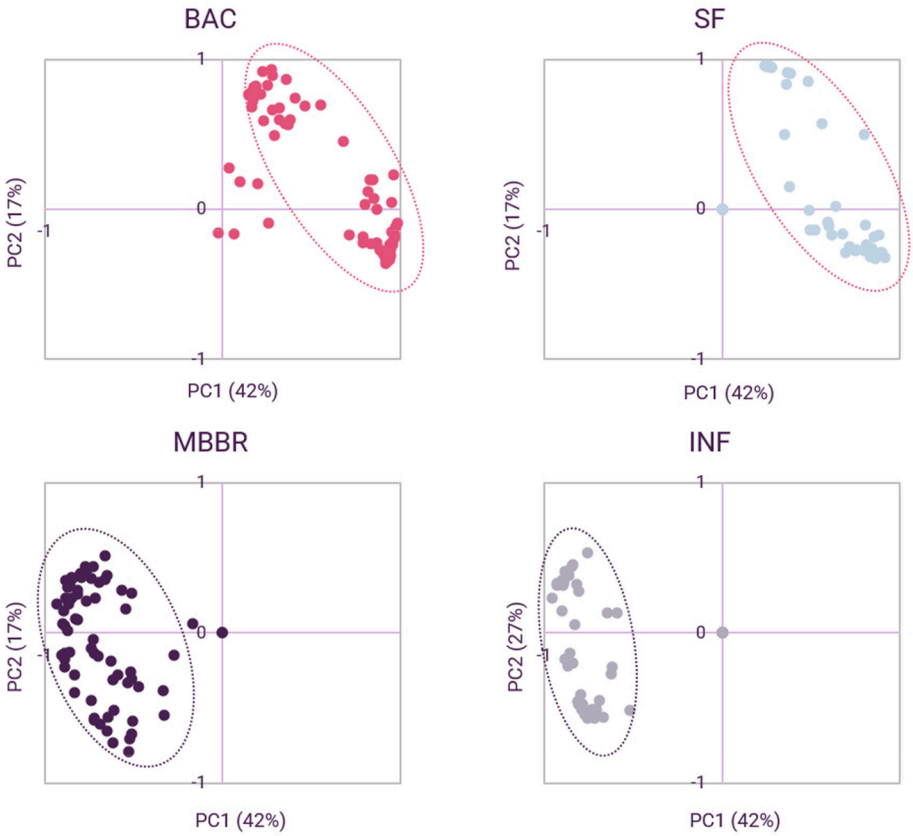

Fig. 6. PCA distribution of microbial data at family level for influent (INF), and each reactor (BAC, MBBR, and SF). Percentages at the axes indicate the amount of variation in microbial data explained.

members of the *Comamonadaceae* are aerobic and heterotrophic bacteria, and some play a role in denitrification (Rosenberg et al., 2014). They are primarily found in soil, freshwater, groundwater, and activated sludge (Rosenberg et al., 2014). Khan et al. (2002) indicated that members of the *Comamonadaceae* predominate under poly(3-hydroxybutyrate-*co*-3-hydroxyvalerate)-acclimated denitrifying conditions (Khan et al., 2002) by using organic compounds as electron donor (Morais et al., 2016). In our study, the gLV model showed that *Comamonadaceae* was one of the most significant taxa in the correlation networks of the microbial community. Mainly it had negative correlations with other taxa in the INF (Fig. 2.b) and MBBR (Fig. 3.b). In contrast, it positively correlated with *Rhodobacteraceae* in BAC (Fig. 4.b) and *Burkholderiaceae* in SF (Fig. 5.b). Furthermore, the significant correlation of the relative abundance of *Comamonadaceae* with the TOC concentration (0.494 at $p < 0.01$) in our MBBR might be related to the available organic compounds as electron donors. Although *Comamonadaceae* had the highest relative abundance in all bioreactors, there was no significant correlation between the removal of organic matter and the concentration of nitrite or nitrate.

In turn, *Xiphinematobacteraceae* (23 %) was the most predominant family in the BAC at the date (2/12: Day/Month) with the highest organic matter removal rate in terms of COD (72 %), TOC (57 %), and UV (61 %). *Xiphinematobacteraceae,* a family within the *Verrucomicrobiota* phylum, can be found in diverse habitats (e.g., freshwater, marine environment, soil, and animal gut (Fuerst, 2019). Most of the genera within the *Xiphinematobacteraceae* have an aerobic and heterotrophic metabolism, but very little is known about their functions. The gLV model indicated a positive correlation between *Xiphinematobacteraceae* and *Sphingomonadaceae* in the BAC. Some species of *Sphingomonadaceae* are associated with biofilm formation - extracellular polymeric substances (EPSs) production (de Vries et al., 2019; Li et al., 2019). Microbial activity in the biofilm of BAC plays a significant role in processing and eliminating organic matter. Nevertheless, the mass transport process, hence the microbial activity, within the biofilm is limited by the thickness of the biofilm (Simpson, 2008). Further research might reveal the relationship between *Xiphinematobacteraceae* and *Sphingomonadaceae* to understand their role in organic matter removal and biofilm formation in BAC, which can be used for harnessing microbial activity in biofilms.

Another abundant family in the BAC was that of the *Mycobacteriaceae,* and its relative abundance significantly correlated with the COD removal rate (0.42 at $p < 0.05$). *Mycobacteriaceae*, a family within the *Actinomycetota,* include aerobic bacteria and are widely distributed in the environment (mainly in soil and water) (Robertson, 2022). Some species of *Mycobacteriaceae* have an essential role in organic matter degradation (Payeur, 2014), which might indicate their role in COD removal. On the other hand, on the day with the highest organic matter removal (2/12: Day/Month), the relative abundance of *Mycobacteriaceae* was 5.63 % in the BAC. Furthermore, the relative abundances of *Mycobacteriaceae* and *Comamonadaceae* were negatively correlated (-0.69 at $p < 0.01$ at SF and 0.43 at $p < 0.01$ at BAC) (see supplementary Tables 1.1 and 1.3, respectively). This might be an indication of competition between members of these two families. Despite this, the gLV model did not reveal a direct correlation between *Mycobacteriaceae* and *Comamonadaceae*, neither for the BAC nor the SF reactor. However, the model showed that *Mycobacteriaceae* was positively correlated with *Acidithiobacillaceae* at SF and MBBR. Members of the *Acidithiobacillaceae* family are capable of iron and/or sulfur oxidation (Kelly and Wood, 2014), and it's tempting to speculate that this positive correlation might suggest a relation between the members of *Mycobacteriaceae* and *Acidithiobacillaceae.* As Li et al. (2022) stated, in the presence of some electron acceptors (e.g. nitrate, sulfate, carbonate, etc.) and intermediate metabolites of micropollutants, particular microbial species can compete or co-exist. Understanding microbial interactions may reveal

unknown mechanisms in micropollutant removal that might be used to increase removal performance by promoting a specific removal mechanism with bioaugmentation of specific microbial species or the addition of a suitable electron acceptor. E-supplementary data for this work can be found in the e-version of this paper online.

On average, the *Rhodobacteraceae* family within the *Proteobacteria* phylum was predominant in the influent and MBBR. In the influent, its relative abundance increased throughout the experiment from 6.5 % to 24 %, whereas it was more constant in the MBBR (Fig. 4.a). Moreover, the gLV model revealed several correlations between *Rhodobacteraceae* and other microbial groups both in the influent (Fig. 2.b) as well as the MBBR (Fig. 4.b), which is another indicator of the high similarity between microbial community profiles in the influent and the effluent of the MBBR. Based on the gLV model, *Rhodobacteraceae* had strong positive correlations between *Flavobacteriaceae*, *Oxalobacteraceae,* and *Burkholderiaceae* in the MBBR (Fig. 4.b). Several members of the *Flavobacteriaceae* were found in municipal wastewater treatment plants and considered to be floc-forming microorganisms due to their ability to produce EPS (Gonzalez-Martinez et al., 2016). Therefore, the positive correlation between *Rhodobacteraceae* and *Flavobacteriaceae* suggested by the gLV model might indicate a syntrophic relation for biofilm formation in the MBBR. Furthermore, the relative abundance of *Rhodobacteraceae* was significantly correlated with the COD removal rate (0.614 at $p < 0.01$) in the MBBR. This observation makes sense as members of the *Rhodobacteraceae* are among the most widely distributed aerobic heterotrophic bacteria in freshwater environments and have a crucial role in carbon and organic sulfur cycling (Pohlner et al., 2019).

Aside from bacteria, *Nitrosopumilaceae*, a family within the archaeal domain, was found in the BAC and SF. Members of the *Nitrosopumilaceae* grow chemolithoautotrophically under anoxic and aerobic conditions (Qin et al., 2016). In parallel with the DO concentration in the BAC and SF, the relative abundance of *Nitrosopumilaceae* was changed: in the BAC, the DO concentration in the middle and bottom of the bioreactor was <0.1 mg/L between days 09.25 and 10.30, while, on these dates, the relative abundance of *Nitrosopumilaceae* changed between 6 % and 26 % (Fig. 3.a). When the DO changed between 0.69 and 2.25 mg/L in the bottom part of the SF, the relative abundance of *Nitrosopumilaceae* was 3 % to 19 % (Fig. 5.a). Moreover, the gLV model indicated a positive correlation between *Nitrosopumilaceae* and *Acidithiobacillaceae* in the BAC (Fig. 3.b). To our knowledge, no relationship between *Nitrosopumilaceae* and *Acidithiobacillaceae* has been stated in the literature, while several representatives of the *Acidithiobacillaceae* family are collaborating with different archaeal species for bioleaching and bio-oxidation (Cárdenas et al., 2010). In light of the synchronic alteration in DO concentration with the relative abundance of *Nitrosopumilaceae* in the BAC, *Acidithiobacillaceae* might have collaborated with *Nitrosopumilaceae* for iron/sulfur oxidation (Kelly and Wood, 2014).

At the genus level (see supplementary Fig. 2), despite the microbial communities differing by the bioreactor type throughout bioreactor operation, the most abundant groups were an unidentified genus within the *Mycobacteriaceae, Candidatus* Xiphinematobacter*, Polynucleobacter, Nordella,* and *Hydrogenophaga*. However, *Roseococcus* was the most predominant group when the highest removal rates were obtained in the MBBR (22 %) and BAC (12 %). *Roseococcus* belongs to the *Acetobacteraceae* family, a genus of obligately aerobic and chemoorganotrophic bacteria (Yurkov, 2015). Their chemoorganotrophic metabolism – utilizing organic compounds as electron donors – might be the reason for the observed correlation of the high carbon removal rate with their high relative abundance (0.89 at $p < 0.05$). The exact functions of members of *Roseococcus* in organic compound degradation await elucidation in future studies, e.g., metatranscriptomics and metaproteomics for the identification of active pathways, prior to testing them for developing a bioaugmentation strategy to enhance organic matter removal efficiency and, therefore, the bioreactor performance in tertiary treatment. E-supplementary data for this work can be found in e-version of this paper online.

As mentioned in the *Materials and Methods* section, the DO differed based on the bioreactor type. The formation of anoxic and oxic zones in bioreactors might cause that observation. Overall, the results of the microbial community profile at the phylum, family, and genus level showed that different microbial metabolisms were possible based on the availability of the various electron acceptors in the bioreactors.

3.2. Effect of flow rate on the microbial community profile

One of the variables for the bioreactor operation was the flow rate. Twelve different flow rates were used during the bioreactor operation, ranging from 0.25 L/h to 4 L/h (Fig. 1.b). During this experiment, the highest organic matter removal was obtained with the lowest flow rate (0.25 L/h), probably due to increasing the contact time of the substrate and microorganisms (van Gijn et al., 2021). Besides bioreactor performance, microbial community composition was monitored regularly. In all bioreactors, the composition of the microbial community changed with increasing flow rate. At the family level, *Mycobacteriaceae* and *Acidithiobacillaceae* were abundant at the lowest flow rate (0.25 L/h). As the flow rate increased to 1 – 2 L/h and 2 – 4 L/h, *Comamonadaceae* and *Xiphinematobacteraceae* became more abundant in the BAC, respectively. Similarly, at the flow rate of 0.25 L/h *Nocardiaceae;* 1 – 2 L/h Comamonadaceae; and 2 – 4 L/h *Rhodobacteraceae,* and *Burkholderiaceae* were abundant, respectively, in the MBBR. In the SF, *Acidithiobacillaceae* at a flow rate of 0.25 L/h and *Comamonadaceae* at a flow rate of 0.5 – 1 L/h were predominant. In addition to the positive effects of a lower flow rate on the growth rate and substrate contact time, it might favor the production of EPS and other natural polymers (Moreira et al., 2013). Thus, a better adaptation capacity of the microbial community in the bioreactor might also play a significant role in the shift of the microbial community composition with respect to the different flow rates (Di Martino, 2018).

Furthermore, van Gijn et al., (2021) showed that the BAC achieved three times higher micropollutant removal (on average 92 % of all MPs were removed) than MBBR and SF. Prior to sampling for the microbial community analysis, micropollutant removal was assessed when the reactors were operated at 1 L/h. The results of our study suggest that flow rate is an important parameter to affect microbial dynamics. Therefore, flow rates might affect the removal of micropollutants as well. For a comprehensive view, in future studies, micropollutant removal capacity should be analyzed in conjunction with the microbial community and the bioreactor operation conditions.

PCA was conducted to analyze how the microbial community changed with the changing flow rate for each bioreactor (see supplementary Fig. 3). At BAC (see supplementary Fig. 3.a) and MBBR (see supplementary Fig. 3.b), microbial communities were clustered based on the low (0.25–1 L/h) and high (1–4 L/h) flow rates. Furthermore, one-way multivariate ANOVA was performed to evaluate possible relationships between microbial composition and organic matter removal rates as a function of time and flow rate. However, no significant relationship was found. E-supplementary data for this work can be found in the e-version of this paper online.

3.3. Sampling strategy to monitor the microbial community profile shift

Microbial community composition and function determine the performance of bioreactors in terms of organic matter removal, and several parameters can alter this profile. Observing an alteration in the microbial community might provide valuable insight into bioreactor performance. To this end, we compared two different sampling strategies for the microbial community, i.e., short-term hourly sampling vs longer-term daily sampling. A Kolmogorov-Smirnov test was conducted with PC1 and PC2 from the PCA of relative abundance data at the family level. This analysis showed that daily sampling (0.276, $p < 0.05$) had a higher significance than hourly sampling (0.186, $p < 0.05$) to observe the evolution of community composition with changing operating conditions. In order to monitor microbial community shifts in studies such

as the one presented here, sampling should take place over longer periods of time with daily samples rather than shorter periods with hourly samples. Despite this, the observation of changes in the microbial community structure depends on several disturbances, including changes in operational and environmental parameters, characterization of the influent and biomass, etc. (Shade et al., 2013). Therefore, the sampling strategy to monitor the microbial community profile shift should be planned based on the observation aim with abiotic and biotic factors.

4. Conclusions

The microbial community dynamics for organic matter removal in three different bioreactors were analyzed. The bioreactor performance was inversely correlated with the similarity of the microbial community profile in the bioreactors to that in the influent. gLV models suggested various interactions in the microbial community in the bioreactors. *Roseococcus* had the strongest correlation with organic matter removal and might be beneficial in developing bioaugmentation strategies to improve bioreactor performance. Applying methods that address microbial functional potential and activity can provide further insights into the role of microorganisms, which can be employed to improve bioreactor performance.

CRediT authorship contribution statement

M. Atasoy: Writing – original draft, Data curation, Visualization. **W. T. Scott Jr.:** Software, Writing – original draft. **K. van Gijn:** Methodology, Investigation. **J.J. Koehorst:** Software, Data curation. **H. Smidt:** Writing – review & editing, Supervision, Funding acquisition. **A.A.M. Langenhoff:** Writing – review & editing, Supervision.

Declaration of Competing Interest

The authors declare that they have no known competing financial interests or personal relationships that could have appeared to influence the work reported in this paper.

Data availability

ENA Project accession number: PRJEB54921

Acknowledgements

The authors thank Laura Vandionant for her support with DNA extraction and library preparation prior to 16S rRNA gene sequencing. The authors acknowledge the Dutch Research Council for its financial contribution to the UNLOCK Project (NWO:184.035.007 and NRGWI.obrug.2018.005).

Appendix A. Supplementary data

Supplementary data to this article can be found online at https://doi.org/10.1016/j.biortech.2023.128659.

References

Barberán, A., Bates, S.T., Casamayor, E.O., Fierer, N., 2012. Using network analysis to explore co-occurrence patterns in soil microbial communities. ISME J. 6, 343–351. https://doi.org/10.1038/ismej.2011.119.

Brenner, D.J., Krieg, N.R., Staley, J.T., Garrity, G.M., 2005. Bergey's Manual® of Systematic Bacteriology, Bergey's Manual® of Systematic Bacteriology. 10.1007/0-387-29298-5.

Bucci, V., Tzen, B., Li, N., Simmons, M., Tanoue, T., Bogart, E., Deng, L., Yeliseyev, V., Delaney, M.L., Liu, Q., Olle, B., Stein, R.R., Honda, K., Bry, L., Gerber, G.K., 2016. MDSINE: Microbial Dynamical Systems INference Engine for microbiome time-series analyses. Genome Biol 17. https://doi.org/10.1186/s13059-016-0980-6.

Caporaso, J.G., Lauber, C.L., Walters, W.A., Berg-Lyons, D., Lozupone, C.A., Turnbaugh, P.J., Fierer, N., Knight, R., 2011. Global patterns of 16S rRNA diversity at a depth of millions of sequences per sample. Proceedings of the National Academy of Sciences 108, 4516–4522. 10.1073/pnas.1000080107.

Cárdenas, J.P., Valdés, J., Quatrini, R., Duarte, F., Holmes, D.S., 2010. Lessons from the genomes of extremely acidophilic bacteria and archaea with special emphasis on bioleaching microorganisms. Appl Microbiol Biotechnol. https://doi.org/10.1007/s00253-010-2795-9.

Chen, L., Zhai, Y., van der Mark, E., Liu, G., van der Meer, W., Medema, G., 2021. Microbial community assembly and metabolic function in top layers of slow sand filters for drinking water production. J Clean Prod 294, 126342. https://doi.org/10.1016/j.jclepro.2021.126342.

de Vries, H.J., Beyer, F., Jarzembowska, M., Lipińska, J., van den Brink, P., Zwijnenburg, A., Timmers, P.H.A., Stams, A.J.M., Plugge, C.M., 2019. Isolation and characterization of Sphingomonadaceae from fouled membranes. NPJ Biofilms Microbiomes 5. https://doi.org/10.1038/s41522-018-0074-1.

Di Martino, P., 2018. Extracellular polymeric substances, a key element in understanding biofilm phenotype. AIMS Microbiol 4, 274–288. https://doi.org/10.3934/MICROBIOL.2018.2.274.

Duc Viet, N., Lee, H., Im, S.J., Jang, A., 2022. Fate, elimination, and simulation of low-molecular-weight micropollutants in an integrated activated carbon-fertiliser drawn osmotic membrane bioreactor. Bioresour Technol 351, 126972. https://doi.org/10.1016/j.biortech.2022.126972.

Fuerst, J.A., 2019. Phylum Verrucomicrobia, Encyclopedia of. Microbiology 551–563. https://doi.org/10.1016/B978-0-12-809633-8.20772-3.

Gonzalez-Martinez, A., Rodriguez-Sanchez, A., Lotti, T., Garcia-Ruiz, M.J., Osorio, F., Gonzalez-Lopez, J., van Loosdrecht, M.C.M., 2016. Comparison of bacterial communities of conventional and A-stage activated sludge systems. Sci Rep 6. https://doi.org/10.1038/srep18786.

Gross, E.L., Leys, E.J., Gasparovich, S.R., Firestone, N.D., Schwartzbaum, J.A., Janies, D. A., Asnani, K., Griffen, A.L., 2010. Bacterial 16S sequence analysis of severe caries in young permanent teeth. J Clin Microbiol 48, 4121–4128. https://doi.org/10.1128/JCM.01232-10.

Kelly, D.P., Wood, A.P., 2014. The Family Acidithiobacillaceae, in: Rosenberg, E., DeLong, E.F., Lory, S., Stackebrandt, E., Thompson, F. (Eds.), The Prokaryotes: Gammaproteobacteria. Springer Berlin Heidelberg, Berlin, Heidelberg, pp. 15–25. 10.1007/978-3-642-38922-1_250.

Khan, S.T., Horiba, Y., Yamamoto, M., Hiraishi, A., 2002. Members of the family Comamonadaceae as primary poly(3-hydroxybutyrate-co-3-hydroxyvalerate)-degrading denitrifiers in activated sludge as revealed by a polyphasic approach. Appl Environ Microbiol 68, 3206–3214. https://doi.org/10.1128/AEM.68.7.3206-3214.2002.

Klindworth, A., Pruesse, E., Schweer, T., Peplies, J., Quast, C., Horn, M., Glöckner, F.O., 2013. Evaluation of general 16S ribosomal RNA gene PCR primers for classical and next-generation sequencing-based diversity studies. Nucleic Acids Res 41, 1–11. https://doi.org/10.1093/nar/gks808.

Kodera, S.M., Das, P., Gilbert, J.A., Lutz, H.L., 2022. iScience Conceptual strategies for characterizing interactions in microbial communities. iScience 25. 10.1016/j.isci.

Koehorst, J.,, Nijsse, B., 2021. Quality assessment, amplicon classification and functional prediction. 10.48546/WORKFLOWHUB.WORKFLOW.154.2.

Li, C., Av-Shalom, T.V., Tan, J.W.G., Kwah, J.S., Chng, K.R., Nagarajan, N., 2021. BEEM-Static: Accurate inference of ecological interactions from cross-sectional microbiome data. PLoS Comput Biol 17. https://doi.org/10.1371/journal.pcbi.1009343.

Li, L., Jeon, Y., Lee, S.H., Ryu, H., Santo Domingo, J.W., Seo, Y., 2019. Dynamics of the physiochemical and community structures of biofilms under the influence of algal organic matter and humic substances. Water Res 158, 136–145. https://doi.org/10.1016/j.watres.2019.04.014.

Li, Z., Ren, L., Qiao, Y., Li, X., Zheng, J., Ma, J., Wang, Z., 2022. Recent advances in membrane biofilm reactor for micropollutants removal: Fundamentals, performance and microbial communities. Bioresour Technol 343, 126139. https://doi.org/10.1016/j.biortech.2021.126139.

Lu, Z., Jing, Z., Huang, J., Ke, Y., Li, C., Zhao, Z., Ao, X., Sun, W., 2022. Can we shape microbial communities to enhance biological activated carbon filter performance? Water Res 212. https://doi.org/10.1016/j.watres.2022.118104.

Mickalide, H., Kuehn, S., 2019. Higher-Order Interaction between Species Inhibits Bacterial Invasion of a Phototroph-Predator Microbial Community. Cell Syst 9, 521–533.e10. https://doi.org/10.1016/j.cels.2019.11.004.

Momeni, B., Xie, L., Shou, W., 2017. Lotka-Volterra pairwise modeling fails to capture diverse pairwise microbial interactions. Elife 6. https://doi.org/10.7554/eLife.25051.001.

Morais, D., Pylro, V., Clark, I.M., Hirsch, P.R., Tótola, M.R., 2016. Responses of microbial community from tropical pristine coastal soil to crude oil contamination. PeerJ 2016, 1–21. https://doi.org/10.7717/peerj.1733.

Moreira, J.M.R., Teodósio, J.S., Silva, F.C., Simões, M., Melo, L.F., Mergulhão, F.J., 2013. Influence of flow rate variation on the development of Escherichia coli biofilms. Bioprocess Biosyst Eng 36, 1787–1796. https://doi.org/10.1007/s00449-013-0954-y.

Nijsse, B., Schaap, P.J., Koehorst, J.J., 2022. FAIR Data Station for Lightweight Metadata Management & Validation of Omics Studies. bioRxiv 2022.08.03.502622. 10.1101/2022.08.03.502622.

Nilsson, F., Ekblad, M., la Cour Jansen, J., Jönsson, K., 2017. Removal of pharmaceuticals with ozone at 10 Swedish wastewater treatment plants. Water Pract Technol 12, 871–881. https://doi.org/10.2166/wpt.2017.087.

Payeur, J.B., 2014. Mycobacterium. Encyclopedia of Food Microbiology: Second Edition 2, 841–853. https://doi.org/10.1016/B978-0-12-384730-0.00229-9.

Pohlner, M., Dlugosch, L., Wemheuer, B., Mills, H., Engelen, B., Reese, B.K., 2019. The majority of active Rhodobacteraceae in marine sediments belong to uncultured genera: A molecular approach to link their distribution to environmental conditions. Front Microbiol 10, 1–16. https://doi.org/10.3389/fmicb.2019.00659.

Poncheewin, W., Hermes, G.D.A., van Dam, J.C.J., Koehorst, J.J., Smidt, H., Schaap, P.J., 2020. NG-Tax 2.0: A Semantic Framework for High-Throughput Amplicon Analysis. Front Genet 10. https://doi.org/10.3389/fgene.2019.01366.

Qin, W., Martens-Habbena, W., Kobelt, J.N., Stahl, D.A., 2016. Candidatus Nitrosopumilaceae. Bergey's Manual of Systematics of Archaea and Bacteria 1–2. https://doi.org/10.1002/9781118960608.fbm00262.

Robertson, R.E., 2022. Mycobacterium spp., in: Encyclopedia of Dairy Sciences. pp. 499–506. 10.1016/b978-0-08-100596-5.22990-9.

Rosenberg, E., De Long, E.F., Lory, S., Stackebrandt, E., Thompson, F., 2014. The prokaryotes: Other major lineages of bacteria and the archaea. The Prokaryotes: Other Major Lineages of Bacteria and The Archaea 1–1028. https://doi.org/10.1007/978-3-642-38954-2.

Shade, A., Gregory Caporaso, J., Handelsman, J., Knight, R., Fierer, N., 2013. A meta-analysis of changes in bacterial and archaeal communities with time. ISME J. 7, 1493–1506. https://doi.org/10.1038/ismej.2013.54.

Simpson, D.R., 2008. Biofilm processes in biologically active carbon water purification. Water Res. https://doi.org/10.1016/j.watres.2008.02.025.

United Nations, 2018. Sustainable Development Goals [WWW Document]. 2018. URL https://sustainabledevelopment.un.org/sdgs.

Valentín-Vargas, A., Toro-Labrador, G., Massol-Deyá, A.A., 2012. Bacterial community dynamics in full-scale activated sludge bioreactors: Operational and ecological factors driving community assembly and performance. PLoS One 7. https://doi.org/10.1371/journal.pone.0042524.

van den Berg, N.I., Machado, D., Santos, S., Rocha, I., Chacón, J., Harcombe, W., Mitri, S., Patil, K.R., 2022. Ecological modelling approaches for predicting emergent properties in microbial communities. Nat Ecol Evol. https://doi.org/10.1038/s41559-022-01746-7.

van Gijn, K., Chen, Y.L., van Oudheusden, B., Gong, S., de Wilt, H.A., Rijnaarts, H.H.M., Langenhoff, A.A.M., 2021. Optimizing biological effluent organic matter removal for subsequent micropollutant removal. J Environ Chem Eng 9, 106247. https://doi.org/10.1016/j.jece.2021.106247.

Yilmaz, P., ..., Glöckner, F.O., "Massive Joint Study" 2011. Minimum information about a marker gene sequence (MIMARKS) and minimum information about any (x) sequence (MIxS) specifications. Nat Biotechnol. 10.1038/nbt.1823.

Yurkov, V.V., 2015. Roseococcus. Bergey's Manual of Systematics of Archaea and Bacteria. 1–4. https://doi.org/10.1002/9781118960608.gbm00887.

Zhang, C., Atashgahi, S., Bosma, T.N.P., Peng, P., Smidt, H., 2022. Organohalide Respiration Potential in Marine Sediments from Aarhus Bay. FEMS Microbiol Ecol 1–13. https://doi.org/10.1093/femsec/fiac073.

Zomorrodi, A.R., Segrè, D., 2016. Synthetic Ecology of Microbes: Mathematical Models and Applications. J Mol Biol. https://doi.org/10.1016/j.jmb.2015.10.019.